Journal of Engineering Science and Technology
Vol. 15, No. 5 (2020) 3265 - 3280

EXPERIMENTAL PREDICTION OF THE DISCHARGE COEFFICIENTS FOR RECTANGULAR WEIR WITH BOTTOM ORIFICES

HUSAM H. ALWAN[1], LAYLA A.M. SALEH[1], FADHIL M. AL-MOHAMMED[2], MUHAMMAD A. ABDULREDHA[1,*]

[1]College of Engineering, Kerbala University, Iraq,
[2]Al-Furat Al-Awsat Technical University, 56001 Kerbala, Iraq
*Corresponding Author: muhammed.r@uokerbala.edu.iq

Abstract

Weir is a hydraulic structure used to regulate and measure flow in irrigation projects. In order to increase the discharge capacity of the weirs and minimize upstream sedimentation, weirs can be combined with gates in one structure. In this paper, the discharge coefficient of the combined device consisting of a rectangular sharp crest weir provided with bottom orifices was studied experimentally and numerically. Ten models with various geometric shapes were suggested, the first was rectangular crested weir without a bottom orifice, while other models varied in number and diameter of the openings. The results showed that the discharge coefficient value for the standard weir was 0.602 while it varied from 0.605 to 0.638 for the weir-orifice. Also, Multilayer Perceptron Artificial Neural Network (MLP-ANN) and Multi Non-Linear regression (MNLR) techniques were used to model the discharge coefficient. The accuracy of these models were tested according to the coefficient of determination (R^2) and relative error. For MLP-ANN model; R^2= 0.91, and relative error =0.47 %, while for MNLR model they were 0.75 and 1.13 %, respectively. The performance of the ANN model shows that the discharge coefficient can be better predicted using artificial intelligent compared to the statistical regression technique.

Keywords: ANN, Composite device, Discharge coefficient, Orifice, Rectangular weir.

1. Introduction

Flow measurements significantly affect the management and planning of agricultural projects. Literature shows various techniques for flow measurements such as weir and orifice which are commonly used in hydraulic engineering practice [1]. Construction of weirs across waterways reduces the upstream velocity, which contributes to the deposition of suspended sediment and decreases the capacity of discharge. One way to improve the performance of weirs is by proposing bottom opening [2, 3]. This combined structure will have similar functions of weir and orifice as flow measurement and control device. For a constant upstream head, the discharge that passes through weir-orifice is higher than the discharge passes over a weir with the same geometry.

Predicting the discharge coefficient is one of the most significant processes for weir design; it depends on the characteristics of flow and channel geometry [4, 5]. So, when the weir is modified from standard to composite, the discharge coefficient (*Cd*) value will be changed to be fit for the new device. In the Literatures, many researchers have studied the issue of the combined weir;

Alhamid et al. [6] proposed a combination device from the V-notch weir and rectangular sluice gate to reduce the sediment problem upstream the weir and to increase its capacity. Different geometric combination models were tested experimentally. Results indicated that the flow through the device is affected by the flow parameters and device geometry. Further, a semi-empirical discharge equation was developed with an absolute error of 4 %.

Abozeid et al. [2] investigated the characteristics of clear overfill weirs provided with bottom openings. They designed nine weir models in a horizontal lab flume and used a range of weir heights, opening diameters, downstream water depths, and discharges to cover three weir flow cases, i.e., free pipe- free weir, submerged pipe - free weir, and submerged pipe- submerged weir. Besides, multiple regression equations were developed based on dimensional analysis to compute discharge for the combined device and all conditions of flow.

Hayawi et al. [7] investigated experimentally the free flow through a combined rectangular weir with three different widths over a semi-circular gate of a constant diameter. Also, the distance below the weir edge and the semi-circular gate were changed three times. It was found that the values of *Cd* ranged from around 0.522 to 0.853 with an average of 0.695. Besides, a multi-regression model was developed to estimate *Cd* for the combined device with a percentage of error ±10 %.

Amery et al. [8] experimentally tested the discharge coefficient of a compound sharp-crested side weir consisting of triangular-rectangular sections with various crest heights and apex angles. They concluded that the discharge coefficient of a triangular-rectangular composite weir depends on the Froude number, weir crest height to the upstream water depth ratio, and the weir length to the upstream depth ratio. Besides, two equations were developed based on experimental data and regression analysis to estimate the discharge coefficient for this compound weir.

In the last decades, artificial intelligence techniques such as Neural Network (ANN), Adaptive Neuro-Fuzzy Inference Systems (ANFIS), Genetic Programming (GP), Group Method of Data Handling (GMDH), and Bayesian networks (BN)

have been employed as a useful and efficient method for modelling and estimating processes related to the water engineering [9, 10].

Due to its ability to solve complex problems that may not have a viable solution, ANN has been widely used in hydraulic engineering and water resources. For example, Nodoushan [11] developed (BN) and ANN models for predicting water quality parameters in Honolulu, Pacific Ocean based on some important characteristics of the water body. The results demonstrated that BN and ANN models can be successfully applied for water quality forecasting in coastal waters.

Al-Ani and Al-Obaidi [12] used ANN and multiple linear regression models for calculating the sediment accumulation in AL-Thawra trunk sewer, Baghdad. They concluded that the ANN model was practical and better suited to the data throughout its range.

As for researches involving discharge coefficients of weirs, and according to recent studies, the ANN provides successful prediction results for different types of weirs compared to conventional regression models. For example, Bilhan et al. [13] used the artificial neural networks to predict the discharge coefficient for triangular -labyrinth side weir in curved channels.

Juma et al. [14] applied (ANN) to determine the discharge coefficient for a hollow- semi-circular crested weir. Parsaie [15] predicted the discharge coefficient for side weir using a multilayer perceptron (MLP-ANN) and radial basis function (RBF-ANN) neural networks.

Eghbalzadeh et al. [16] used three different ANN models, i.e., feed-forward backpropagation, generalized regression neural, and radial basis function networks to forecast the discharge coefficient for flow through both circular and square shapes of sharp-crested side orifices.

Ansari et al. [17] established a generalized model for estimating the coefficient of discharge of compound sharp-crested weir using ANN-RBF. Norouzi et al. [18] investigated the performance of (MLP-ANN), (RBF-ANN) and support vector machines in estimating the discharge coefficient of trapezoidal labyrinth weir with quarter-round crests using.

According to our knowledge, the estimation of a discharge coefficient for rectangular weir provided with more than one bottom orifice using an artificial neural network has rarely been investigated. Thus, the objective of this paper is to develop the ANN model to predict the discharge coefficient for the weir-orifice device based on experimental data. Also, the performance of the ANN model is compared with the traditional regression approach.

The remainder of this paper is structured as follows; materials and methods, including experimental setup and data processing, are defined in Section 2. The techniques used for data modelling are specified in Section 3. Results and discussion are presented and discussed in Section 4. The flowchart of research methodology is illustrated in Fig. 1.

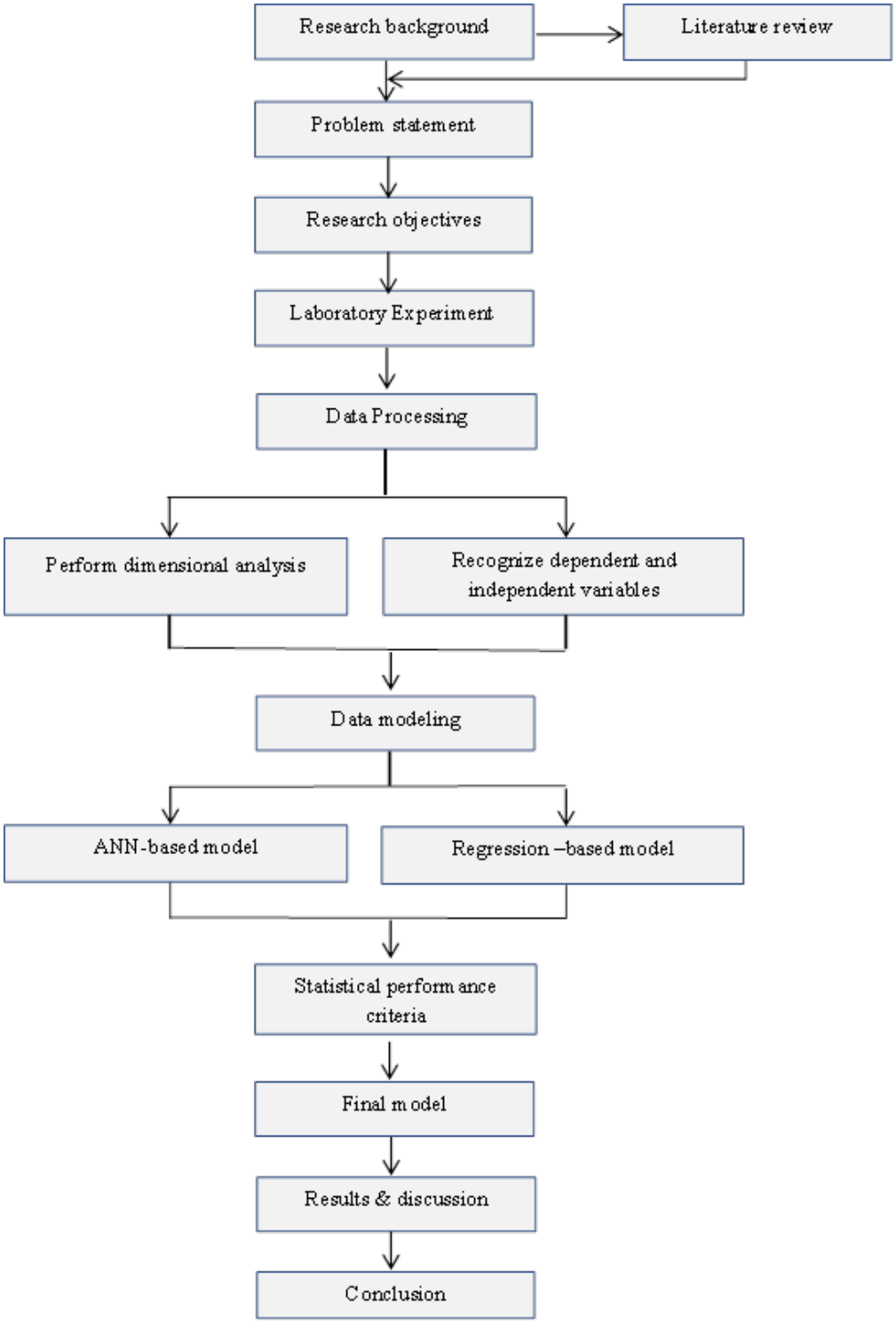

Fig. 1. Flowchart of the research methodology.

2. Experimental Procedure

2.1. Experimental setup

The experiments were carried out in a hydraulic bench channel of length 70 cm, width 25 cm and height 16.6 cm as shown in Fig. 2. The bench had a locked-loop water system and the main tank under the bench flume with a capacity of 1.2 m^3 was located below the bench flume. Water was delivered from the main tank to the upstream inlet tank of 0.2 m^3 capacity by a centrifugal pump with a rated capacity of 40 lps.

During all the tests the bench bed was maintained at a horizontal slope. Also, a movable carriage with an electronic vernier of 0.01 mm accuracy was kept at a horizontal slope. Ten models of notches were made from 4 mm thick acrylic glass plates, the first one was a rectangular crested weir without a bottom orifice and considered standard. A sample of the proposed combined device is shown in Fig. 3. The descriptions of the experimental models are given in Table 1.

For all models, the lower edge of the rectangular weir was 4.25 cm from the centre of the orifices. The experimental procedure used is summarized below.

1- Installing the model in the specific position on a hydraulic bench channel.
2- Supplying the channel with a specific discharge of water by adjusting a control valve in the bench supply line.
3- For each discharge, after waiting a few minutes and when the discharge and its hydraulic measurements became stable, water depth measurements were taken at a distance of 30 cm upstream of the weir using vernier.
4- Recording, over the period, the volume of water stored in the bench tank. The actual discharge was calculated using the volume method, i.e., $Q_{act.}$ = volume/time.
5- The discharge was changed and several readings were recorded for each test.
6- The model was changed according to Table 1; repeat the steps from 2 to 4.

Fig. 2. The laboratory channel and volume measuring tank.

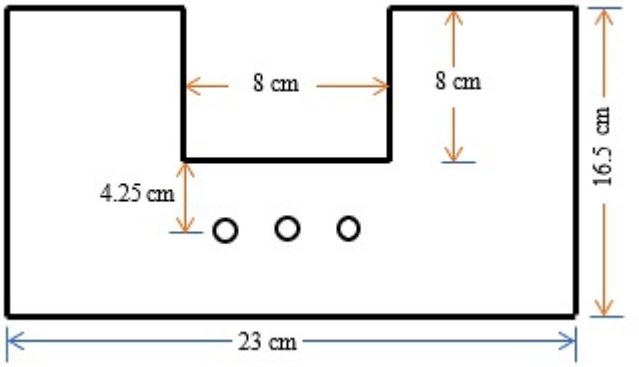

Fig. 3. Sample of proposed combined device.

Table 1. The characteristics of experimental models.

Model No.	Description
1	Standard weir
2	Standard weir with one central orifice of 0.5 cm diameter
3	Standard weir with two orifices of 0.5 cm diameter
4	Standard weir with three orifices of 0.5 cm diameter
5	Standard weir with one orifice of 0.75 cm diameter
6	Standard weir with two orifices of 0.75 cm diameter
7	Standard weir with three orifices of 0.75 cm diameter
8	Standard weir with one orifice of 1 cm diameter
9	Standard weir with two orifices of 1 cm diameter
10	Standard weir with three orifices of 1cm diameter

2.2. Theoretical background:

The general forms of theoretical discharge passing through rectangular weir and orifice are [19-21]:

$$Q_{the.w} = \frac{2}{3} b\sqrt{2g} \quad H^{1.5} \tag{1}$$

$$Q_{the.o} = \frac{\pi}{4} D^2 \sqrt{2gh} \tag{2}$$

where $Q_{the.w}$ is theoretical discharge passing over a rectangular crest weir, b is weir width, g is the gravitational acceleration, H is upstream head over the bottom edge of rectangular weir, $Q_{the.o}$ is theoretical discharge through the orifice, D is orifice diameter, and his the head above the orifice centre to the water surface level.

Model geometry and drawdown effects mean that the actual discharge is less than theoretical, thus Eqs. (1) and (2) must be multiplied by a discharge coefficient as shown:

$$Q_{act.w} = Cd_w \frac{2}{3} b\sqrt{2g} \quad H^{1.5} \tag{3}$$

$$Q_{act.o} = Cd_o \frac{\pi}{4} D^2 \sqrt{2gh} \tag{4}$$

where $Q_{act.w}$ is actual discharge passing over a sharp-crested rectangular weir, Cd_w is weir discharge coefficient, $Q_{act.o}$ is actual discharge through the orifice, and C_{do} is orifice discharge coefficient.

To compute the discharge through a suggested combined weir, the equations of discharge over the rectangular weir and through the orifice are added together. The actual discharge passing through the composite device will be:

$$Q_{act.c} = Cd_w \frac{2}{3} b\sqrt{2g}\ \ H^{1.5} + Cd_o \frac{\pi}{4} D^2 \sqrt{2gh} \quad (5)$$

where $Q_{act.c}$ is the actual discharge for the composite device. It is important to recognize the difference between the head of orifice (h) and the head of weir (H). Eq. (5) can be rewritten to be in this format:

$$Q_{act.c.} = Cd\ Q_{the.c.} \quad (6)$$

where Cd is the discharge coefficient of a combined weir, $Q_{the.c.}$ is the theoretical discharge of combined weir; i.e.,

$$Q_{the.c.} = Q_{the.w} + Q_{the.o.} \quad (7)$$

2.3. Dimensional analysis

The dimensional analysis can be used to determine the physical relationship between discharge and other related parameters [2, 21]. Thus, the relationship between the discharge coefficient of the proposed wire-orifice device and the effective parameters can be expressed as follows:

$$Cd = f(g, \rho, \mu, H, B, d, n, h) \quad (8)$$

where Cd is discharge coefficient, g is gravitational acceleration, ρ is water mass density, μ is the dynamic viscosity of water, H is total head over the weir crest, B is weir width, d is orifice diameter, n is the number of openings, and h is the distance measured from centre of the orifice to the water surface.

The parameters B was considered to be constant in this study and h varied with H. By applying Buckingham's-theorem and using ρ, g and d as a repeating variable, the following function is obtained:

$$Cd = f(\frac{\rho d\sqrt{2gH}}{\mu}, \frac{H}{d}, n) \quad (9)$$

The term $(\frac{\rho d\sqrt{2gH}}{\mu})$ represents Reynolds number (Re) that can be ignored in the open channel as the flow motion is primarily controlled by the boundary friction and force of gravity, besides most physical experiments are usually performed using Froude similitude, which requires a significantly smaller laboratory Reynolds numbers than the corresponding prototype flows [22, 23]. So, Eq. (9) can be reduced as follows:

$$Cd = f(\frac{H}{d}, n) \quad (10)$$

In this study, non-dimensional parameters of Eq. (10) were used as input and output variables to develop artificial neural network ANN and multiple non-linear regression (MNLR) models using SPSS statistical software. The data was divided into two sets: 80 % to build a model and 20 % to evaluate its performance.

3. Discharge Coefficient Models

3.1. Artificial neural network model (ANN)

Artificial Neural Network (ANN) is a data modelling tool capable of capturing and representing complex input and output relationships. This technique can perform an

intelligent task similar to those produced by the human brain [9]. The Multilayer Perceptron (MLP) with the back-propagation -algorithms are the most commonly used neural network model which requires the desired input and output data to learn. The purpose of this network is to build a model that correctly maps the input to the output using historical data so that the developed model can later produce the output when the desired output is not available [24-26]. The structure of the artificial neural networks contains three parts: the input layer, hidden layer, and output layer. Each of the input and hidden layers has an additional unit called the bias unit *(ß)*, ANN parts are linked to each other by nodes or neurons to form a parallel distributed processing system [27, 28]. In the MLP-ANN process, the input data are fed into the input layer and multiplied by weights of interconnection as they pass from the input layer to the hidden layer. Weighted inputs are summed with a bias *(ß)* value within the hidden layer and processed by a nonlinear function, usually the hyperbolic tangent. As the processed data leaves the hidden layer, it multiplies by other interconnection weights and finally, it processed within the output layer to produce the model output. In the backpropagation technique, the input data is repeatedly offered to the neural network. The neural network output is compared to the target output with each presentation and an error is determined. This error is then returned to the neural network (i.e., propagated back) and used for weight correction. This process continues until an input-output mapping can be achieved with a minimum possible error. The above process is called training or learning [29-31].

The ANN model was developed in the study using IBM SPSS v.25 software, and the input parameters were: the ratio of head to orifice diameter (*H/d*) and the number of the orifice (*n*), while the discharge coefficient of the combined weir (*Cd*) was adopted as the output variable. The data set were portion into three sets; training, testing and validation. The training sample contains the data records applied for training the neural network; some percentage of cases in the dataset must be selected for the training sample to build the model. The test sample is a separate set of data used to record the errors during the training process in order to prevent over-training. The holdout (validation) sample is another independent set of the data records needed to estimate the final neural network model. The error for the holdout sample provides an "honest" evaluation of the model ability for prediction because these data have not been used in model creation.

3.2. Multiple Non-Linear Regressions (MNLR)

Regression analysis is one of the most commonly used techniques for expressing the dependency of the response variable on the several independent variables. Unlike traditional linear regression, which is limited to the estimation of simple linear models, nonlinear regression can be used for models with an arbitrary relation between dependent and independent variables [32]. For multiple non-linear regression, observational data are represented by a function that is a non-linear combination of model parameters and depends on more than one independent variable. The general form of the multiple nonlinear relations is considered to be [33]:

$$Y = a_0 . (X_1)^{a_1} . (X_2)^{a_2} \dots \dots \dots (X_n)^{a_n} \quad (11)$$

where Y is the predicted value corresponding to the dependent variables, a_0 is the intercept, X_1, X_2, X_n are the independent variables, and a_1, a_2, a_n are the regression coefficients of independent variables.

4. Results and Discussions

4.1. Discharge coefficient

Values of the discharge coefficient *Cd* were calculated for the standard weir (model 1) for various flow rates using Eq. (3), and the average value was about 0.602 which is within the acceptable values. The relation between the head and the actual discharge is illustrated in Fig. 4. The discharge coefficients for other models were computed using Eqs. (1), (2), and (6), respectively. The result shows that the *Cd* for the weir-orifice device varies from 0.605 to 0.638 with an average value of 0.618 and standard deviation of 0.0099. Increasing discharge coefficients of the composite device imply that the addition of bottom orifice to the standard wire contributes to an improvement in its efficiency. Table 2 explains the details of the tests.

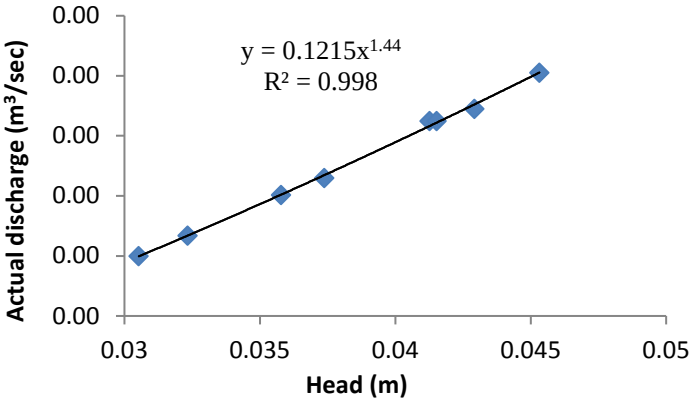

Fig. 4. The relation between the water head and actual discharge.

Table 2. The statistical results of the models' tests.

Model	Parameter	*H*(m)	$Q_{act.c}$ (m^3/s)	$Q_{the.w}$ (m^3/s)	$Q_{the.o}$ (m^3/s)	$Q_{the.c}$ (m^3/s)	*Cd*
2	Max.	4.69E-02	1.50E-03	2.40E-03	2.60E-05	2.42E-03	6.20E-01
	Min	2.20E-02	4.80E-04	7.69E-04	2.21E-05	7.91E-04	6.05E-01
	Average	3.49E-02	9.80E-04	1.59E-03	2.41E-05	1.61E-03	6.08E-01
	St.dev.	8.87E-03	3.59E-04	5.79E-04	1.39E-06	5.80E-04	4.63E-03
3	Max.	4.33E-02	1.39E-03	2.13E-03	5.09E-05	2.18E-03	6.38E-01
	Min.	2.13E-02	4.85E-04	7.35E-04	4.39E-05	7.78E-04	6.19E-01
	Average	3.44E-02	9.93E-04	1.53E-03	4.82E-05	1.58E-03	6.27E-01
	St.dev.	7.91E-03	3.23E-04	5.05E-04	2.50E-06	5.07E-04	7.43E-03
4	Max.	4.76E-02	1.58E-03	2.45E-03	7.83E-05	2.53E-03	6.25E-01
	Min.	3.42E-02	9.65E-04	1.49E-03	7.22E-05	1.57E-03	6.05E-01
	Average	4.06E-02	1.24E-03	1.94E-03	7.52E-05	2.02E-03	6.13E-01
	St.dev.	5.04E-03	2.33E-04	3.59E-04	2.29E-06	3.62E-04	7.45E-03
5	Max.	4.53E-02	1.43E-03	2.27E-03	5.79E-05	2.33E-03	6.23E-01
	Min.	2.43E-02	5.72E-04	8.93E-04	5.05E-05	9.44E-04	6.06E-01
	Average	3.61E-02	1.04E-03	1.64E-03	5.48E-05	1.70E-03	6.12E-01
	St.dev.	6.99E-03	2.85E-04	4.65E-04	2.46E-06	4.68E-04	6.31E-03
6	Max.	4.39E-02	1.42E-03	2.17E-03	1.15E-04	2.29E-03	6.36E-01
	Min.	3.09E-02	8.40E-04	1.28E-03	1.06E-04	1.39E-03	6.06E-01
	Average	3.67E-02	1.12E-03	1.67E-03	1.10E-04	1.78E-03	6.28E-01
	St.dev.	4.45E-03	1.99E-04	3.04E-04	3.12E-06	3.09E-04	1.02E-02
7	Max.	4.30E-02	1.45E-03	2.11E-03	1.72E-04	2.28E-03	6.37E-01
	Min.	3.20E-02	9.20E-04	1.35E-03	1.60E-04	1.51E-03	6.06E-01
	Average	3.77E-02	1.17E-03	1.73E-03	1.66E-04	1.90E-03	6.17E-01

	St.dev.	3.88E-03	1.76E-04	2.67E-04	4.26E-06	2.69E-04	1.06E-02
8	Max.	4.32E-02	1.37E-03	2.12E-03	1.02E-04	2.22E-03	6.30E-01
	Min.	3.03E-02	8.14E-04	1.24E-03	9.38E-05	1.34E-03	6.07E-01
	Average	3.67E-02	1.09E-03	1.67E-03	9.78E-05	1.76E-03	6.17E-01
	St.dev.	4.69E-03	2.12E-04	3.22E-04	2.93E-06	3.22E-04	9.74E-03
9	Max.	4.53E-02	1.52E-03	2.28E-03	2.06E-04	2.48E-03	6.19E-01
	Min.	2.94E-02	8.35E-04	1.19E-03	1.86E-04	1.38E-03	6.06E-01
	Average	3.66E-02	1.14E-03	1.66E-03	1.95E-04	1.86E-03	6.12E-01
	St.dev.	5.56E-03	2.36E-04	3.79E-04	6.93E-06	3.83E-04	5.01E-03
10	Max.	4.41E-02	1.54E-03	2.18E-03	3.07E-04	2.49E-03	6.36E-01
	Min.	2.64E-02	8.20E-04	1.02E-03	2.74E-04	1.29E-03	6.17E-01
	Average	3.81E-02	1.29E-03	1.77E-03	2.96E-04	2.07E-03	6.24E-01
	St.dev.	6.27E-03	2.59E-04	4.12E-04	1.18E-05	4.26E-04	7.05E-03

4.2. Multiple nonlinear regression model

Multiple Nonlinear Regression (MNLR) analysis was conducted to correlate the dimensionless parameters shown in Eq. (10). About 80 % of the data set was used for building the model and 20 % for validation. It is necessary to mention that the same validation data was used for both ANN and MNLR models so that the results of both models can be compared. An empirical equation was developed to compute the discharge coefficient of rectangle weir with a bottom orifice, which can be expressed as follows;

$$Cd = 0.000275\left(\frac{H}{d}\right)^3 - 0.00493\left(\frac{H}{d}\right)^2 + 0.028 * \left(\frac{H}{d}\right) - 0.007n^2 + 0.03n + 0.54 \quad (12)$$

The average relative error for the validation data set was about 1.13 % and R^2= 0.75 as shown in Fig. 5. It is widely accepted among statisticians that a coefficient of determination more than 70 % is quite satisfactory. For example, Barbara stated that a model with a coefficient of determination of 70 % provide reliable prediction and Pallant confirmed that 70 % or more is adequate among statistical researches. Besides, it is hard to obtain a higher coefficient of determination with a low number of prediction variables [34, 35]. Thus, R^2 of 75 % obtained in this study using two predictors (*H/d*, *n*) can be considered acceptable. Besides, an increase in the number of orifices has contributed to a more complicated relationship and, thus, an artificial intelligence approach can be used to model this relationship.

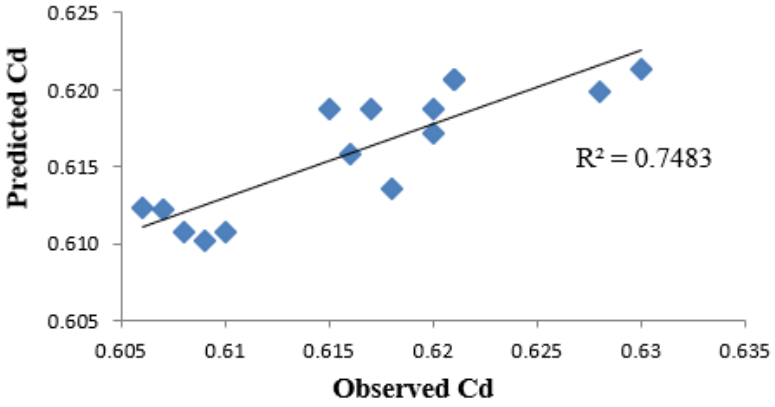

Fig. 5. The scatter plot of the MNLR model for the validation set.

4.3. MLP- ANN model

In this study, approximately 80 % of the data were used to build the ANN model while the remaining 20 % were detained to validate the accuracy of the developed model. An essential step to improve the training process is to rescale the input data to an appropriate scale to reduce the size of the input space. So, a standardized method was applied. The appropriate model was selected after trying different ANN structures. The ANN network with one hidden layer is used and the number of hidden nodes was selected using trial and error method. The hyperbolic tangent and identity activation functions were used for the hidden and output nodes, respectively. The training process for ANN networks was stopped when the relative error between observed and calculated data was too small. Thus, it was found that the most acceptable MLP-ANN model for relating *Cd* with $\left(\frac{H}{d}, n\right)$ consists of an input layer with two nodes, one hidden layer with five nodes, and the output layer of one node. The hyperbolic tangent and identity functions were used for the hidden and the output layers, respectively as shown in Fig. 6. The estimation values of network weights (*w*) for the ANN model are illustrated in Table 3.

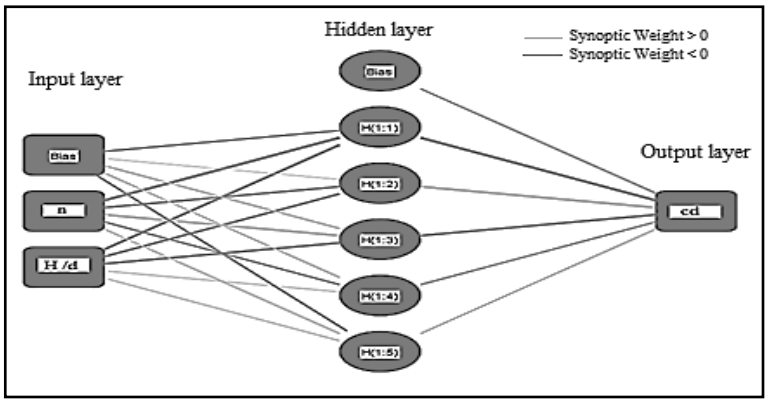

Fig. 6. The structure of the developed MLP-ANN model.

Table 3. Parameters of the proposed MLP-ANN model.

		Predicted					
	Predictor	**Hidden Layer**					**Output Layer**
		H(1:1)	*H*(1:2)	*H*(1:3)	*H*(1:4)	*H*(1:5)	*Cd*
Input Layer	**(Bias)**	-0.526	0.031	0.370	0.332	-0.378	
	N	-2.649	-0.714	1.462	-0.343	0.308	
	H/d	-1.228	-0.743	-1.064	0.039	0.144	
Hidden Layer	**(Bias)**						-0.193
	***H*(1:1)**						-2.117
	***H*(1:2)**						2.010
	***H*(1:3)**						-0.756
	***H*(1:4)**						-0.222
	***H*(1:5)**						-0.027

The mathematical expression of the MLP- ANN model in the form of matrix equation can be given as:

$$Cd = \sum_{j=1}^{5}(w_j * (tanh\left(\sum_{i=1}^{2}(w_{i,j} * x_i) + \beta_i\right))) + \beta \quad (13)$$

where w_j is the weight that connected j^{th} hidden neuron with output layer node, $w_{i,j}$ is the weight linking the i^{th} node of the input layer with the j^{th} hidden layer node,

x_i is the node of the input layer, i.e., independent variables, β_i is the bias value of the j^{th} node in the hidden layer, and β is the bias value of the output layer node.

Table 4 shows the information about the results of applying the MLP- ANN network to the training, testing and holdout sample. The sum-of-squares error is presented because the output layer has scale dependent variables. The network tries to minimize the sum-of-squares error function during the training process. One sequential step with no decrease in error was used as a stopping rule. The relative error for each scale-dependent variable is the ratio of the sum-of-squares error for the dependent variable to the sum-of-squares error for the "null" model, in which the mean value of the dependent variable is used as the predicted value for each case.

Table 4. MLP-ANN model summary.

Training	Sum of Squares Error	14.435
	Relative Error	0.642
Testing	Sum of Squares Error	3.043
	Relative Error	0.526
Validation	Relative Error	0.471

The average of relative error is somewhat convergent through training (0.642), testing 0.526 and holdout (0.471) samples, giving us trust that the model has not been overtrained and the error found by the network in future cases will be similar to the error recorded in Table 4. The lowest relative error was for the validation set, which indicates the accuracy of the model as this set was not included in the building process. The coefficient of determination between observed and predicted *Cd* for (validation) data was R^2=0.91 as shown in Fig. 7.

The ANN model presented in this research provides good results compared to the same studies related to the artificial neural network. For example, the model developed by Al-Suhili and Shwana [36] to predict the discharge coefficient of the weir with a rectangular bottom opening provided a correlation coefficient of 0.88. Whereas R^2 was 0.98 for weir-gate discharge coefficient model developed by Balouchi and Rakhshandehroo [37].

In general, Artificial Neural Networks perform better than the traditional regression method in predicting the discharge coefficient. Although the regression methods are well known and simple to use, their forecasting abilities are decreased as the related data become more complex while the ANN can better estimate when trained with appropriate information

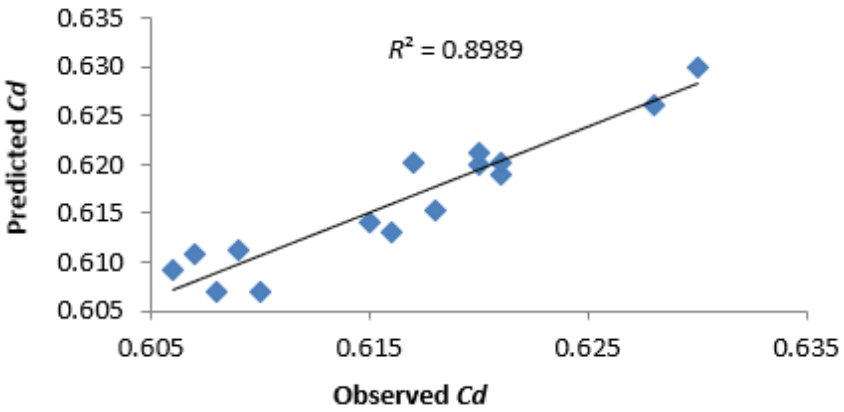

Fig. 7. The scatter plot of the MLP- ANN model for the validation set.

5. Conclusion

In this study, the standard rectangular sharp crest weir was modified by adding bottom opening and the discharge coefficient was studied experimentally for nine models. Also, the Artificial Neural Network (MLP-ANN) and Multi Non-Linear regression MNLR techniques were used to model and predict the discharge coefficient of the weir- orifice composite device. The following results obtained:

- The discharge coefficient for standard weir was 0.602 while this value was increased for composite weir- orifice models to be about 0.618 with a standard division of 0.0099.
- The MLP-ANN model had (2, 5, 1) structure and the coefficient of determination between observed and predicted *Cd* for validation data was R^2=0.91, and relative error 0.471.
- The coefficient of determination between observed and predicted *Cd* for MNLR validation data was R^2=0.75, and relative error 1.13C %.
- The performance of the ANN model shows that the *Cd* could be better predicted using the ANN technique compared to that obtained using the traditional regression analyses

Nomenclatures

B	Weir width, m.
Cd	Discharge coefficient of the combined weir.
d	Orifice diameter, m
H	Total head over the weir crest, m.
h	the distance measured from centre of the orifice to the water surface, m.
n	Number of openings
$Q_{act.}$	Actual discharge, m^3/sec.
$Q_{the.}$	Theoretical discharge, m^3/sec.
Re	Reynolds number

Abbreviations

MLP-ANN	Multilayer Perceptron Artificial Neural Network
MNLR	Multi Non Linear regression

References

1. Alhamid, A.A. (1999). Analysis and formulation of flow through combined V-notch-gate-device. *Journal of Hydraulic Research*, 37(5), 697-705.
2. Abozeid, G; Mohamed, H.I.; and Shehata, S.M. (2010). Hydraulics of clear overfall weirs with bottom-openings. *Ain Shams Engineering Journal*, 1(2), 115-119.
3. Parsaie, A.; Haghiabi, A.H.; Saneie, M.; and Torabi, H. (2017). Predication of discharge coefficient of cylindrical weir-gate using adaptive neuro fuzzy inference systems (ANFIS). *Frontiers of Structural and Civil Engineering*, 11(1), 111-122.
4. Kumar, S.; Ahmad, Z.; and Mansoor, T. (2011). A new approach to improve the discharging capacity of sharp-crested triangular plan form weirs. *Journal of Flow Measurement and Instrumentation*, 22(3), 175-180.
5. Alwan, H.H.; and Al-Mohammed, F.M. (2018). Discharge coefficient for rectangular notch using a dimensional analysis technique. *IOP Conference Series: Materials Science and Engineering*, 433(1), 012015
6. Alhamid, A.A.; Negm, A.Z.; and Albrahim, A.M. (1997). Discharge equation for proposed self - cleaning device. *Journal of King Saud University - Engineering Sciences*, 9(1), 13-24.
7. Hayawi, H.A.; Hayawi, A.M.; and Alniami, A.A. (2009). Coefficient of discharge for a combined hydraulic measuring device. *Journal of Al-Rafidain Engineering*, 17(6), 92-100.
8. Amery, M.; Ahmadi, A.; and Dehghani, A.A. (2015). Discharge coefficient of compound triangular-rectangular sharp-crested side weirs in subcritical flow conditions. *Journal of Flow Measurement and Instrumentation*, 45, 170-175.
9. Salmasi, F.; Yildirim, G.; Masoodi, A.; and Parsamehr, P. (2013). Predicting discharge coefficient of compound broad-crested weir by using genetic programming (GP) and artificial neural network (ANN) techniques. *Arabian Journal of Geosciences*, 6(7), 2709-2717.
10. Khorchani, M.; and Blanpain, O. (2018). Development of a discharge equation for side weirs using artificial neural networks. *Journal of Hydroinformatics*, 7(1), 31-39.
11. Nodoushan, E.J. (2018). Monthly forecasting of water quality parameters within Bayesian networks: A case study of Honolulu, Pacific Ocean. *Civil Engineering Journal*, 4(1), 188-199.
12. Al-Ani, R.R.A.; and Al-Obaidi, B.H.K. (2019). Prediction of sediment accumulation model for trunk sewer using multiple linear regression and neural network techniques. *Civil Engineering Journal*, 5(1), 82-92.
13. Bilhan, O.; Emiroglu, M.E.; and Kisi, O. (2011). Use of artificial neural networks for prediction of discharge coefficient of triangular labyrinth side weir in curved channels. *Advances in Engineering Software*, 42(4), 208-214.

14. Juma, I.A.; Hussein, H.H.; and Al-Sarraj, M.F. (2014). Analysis of hydraulic characteristics for hollow semi-circular weirs using artificial neural networks. *Journal of Flow Measurement and Instrumentation*, 38, 49-53.
15. Parsaie, A. (2016). Predictive modeling the side weir discharge coefficient using neural network. *Modeling Earth Systems and Environment Journal*, 2(2), 1-11.
16. Eghbalzadeh, A.; Javan, M.; Hayati, M.;and Amini, A. (2016). Discharge prediction of circular and rectangular side orifices using artificial neural networks. *Korean Society of Civil Engineers (KSCE) Journal of Civil Engineering*, 20(2), 990-996.
17. Ansari, M.A.; Hussain, A.; Shariq, A.; and Alam, F. (2019). Experimental and numerical studies for estimating coefficient of discharge of side compound weir. *Canadian Journal of Civil Engineering*, 46(10), 887-95.
18. Norouzi, R.; Daneshfaraz, R.; and Ghaderi, A. (2019). Investigation of discharge coefficient of trapezoidal labyrinth weirs using artificial neural networks and support vector machines. *Journal of Applied Water Science*, 9(7), 148.
19. AbdelHalim, N.A.; Sherif, M.M.; and El-Zaher, A.S. (1991). On the Fayoum weirs with orifices. *Journal of Engineering Applied for Science*, 38(5), 893-904.
20. Jalil, S.A.; and Sarhan, S.A. (2013). Experimental study of combined oblique weir and gate structure. *ARPN Journal of Engineering and Applied Sciences*, 8(4), 306-315.
21. Mohamed, H.I.; Abozeid, G.; and Shehata, S.M. (2010). Hydraulics of clear and submerged overfall weirs with bottom circular-openings. *Ain Shams Engineering Journal*, 1(2), 115-119.
22. Chanson, H. (2004). *Environmental hydraulics for open channel flows*. Buttherwoth, Heinemann: Elsevier Ltd.
23. Radecki-Pawlik, A.; Pagliara, S.; and Hradecky, J. (2017). *Open channel hydraulics, river hydraulic structures and fluvial geomorphology: For engineers, geomorphologists and physical geographers* (1st ed.). Boca Raton: CRC Press.
24. Majeed S.A.; Saleh L.A.; and Aswed, G.K. (2018). Modeling the water quality index and climate variables using an artificial neural network and non-linear regression. *International Journal of Engineering & Technology*, 7(3), 1346-1351.
25. Maliki, O.S.; Agbo, A.O.; Maliki, A.O.; Ibeh, L.M.; and Agwu, C.O. (2011) Comparison of regression model and artificial neural network model for the prediction of electrical power generated in Nigeria. *Advances in Applied Science Research*, 2(5), 329-339.
26. El-Belasy, A.M. (2013). Developing Formulae for combined weir and orifice (case study: EL-Fayoum weirs). *Alexandria Engineering Journal*, 52(4), 763-768.
27. Saleh, L.A. (2018). Studying the seepage phenomena under a concrete dam using SEEP/W and Artificial Neural Network models. *IOP Conference Series: Materials Science and Engineering*, 433, 1-15.
28. Mahmoudi, J.; Arjomand, M. A.; Rezaei, M., and Mohammadi, M. H. (2016). Predicting the earthquake magnitude using the multilayer perceptron neural network with two hidden layers. *Civil engineering journal*, 2(1), 1-12.

29. Shahin, M.A.; Jaksa, M.B.; and Maier, H.R. (2008). State of the art of artificial neural networks in geotechnical engineering. *Electronic Journal of Geotechnical Engineering*, 8(1), 1-26.
30. Aswed, G.K. (2016). Productivity estimation model for bracklayer in construction projects using neural network. *Al-Qadisiyah Journal of Engineering Sciences*, 9(2), 93-183.
31. Saleh, L.A.; Majeed, S.A.; and Alnasrawi, F.A. (2019). Numerical study of the bridge pier scour using gene expression programming. *Journal of Applied Water Engineering and Research*, 7(4), 287-294.
32. Abbas, S.H; Khudair, B.H; And Jaafar, M.H. (2019). Water quality assessment and total dissolved solids prediction for Tigris river in Baghdad city using mathematical models. *Journal of Engineering Science and Technology*, 14(6), 3337 - 3346.
33. Yasar, A.; Bilgili, M.; and Simsek, E. (2012). Water demand forecasting based on stepwise multiple nonlinear regression analysis. *Arabian Journal for Science and Engineering*, 37, 2333-2341.
34. Tabachnick, B. G.; Fidell, L. S.; and Ullman, J. B. (2007). *Using multivariate statistics* (vol. 5). Boston, MA: Pearson.
35. Pallant, J. (2013). *SPSS survival manual*. United Kingdom: McGraw-Hill Education.
36. Al-Suhili, R.H.; and Shwana, A.J. (2013). Prediction of the discharge coefficient for a Cipolletti weir with rectangular bottom opening. *Journal of Engineering Research and Applications*, 4(1), 80-89.
37. Balouchi, B.; and Rakhshandehroo, G. (2018). Using physical and soft computing models to evaluate discharge coefficient for combined weir-gate structures under free flow conditions. *Iranian Journal of Science and Technology, Transactions of Civil Engineering*, 42(4), 427-438.